

Regular article

Long-range and short-range Coulomb correlation effects as simulated by Hartree–Fock, local density approximation, and generalized gradient approximation exchange functionals

Victor Polo, Jürgen Gräfenstein, Elfi Kraka, Dieter Cremer

Department of Theoretical Chemistry, Göteborg University, Reutersgatan 2, 413 20 Göteborg, Sweden

Received: 25 May 2002 / Accepted: 7 October 2002 / Published online: 21 January 2003
© Springer-Verlag 2003

Abstract. Exchange functionals used in density functional theory (DFT) are generally considered to simulate long-range electron correlation effects. It is shown that these effects can be traced back to the self-interaction error (SIE) of approximate exchange functionals. An analysis of the SIE with the help of the exchange hole reveals that both short-range (dynamic) and long-range (nondynamic) electron correlation effects are simulated by DFT exchange where the local density approximation (LDA) accounts for stronger effects than the generalized gradient expansion (GGA). This is a result of the fact that the GGA exchange hole describes the exact exchange hole close to the reference electron more accurately than the LDA hole does. The LDA hole is more diffuse, thus leading to an underestimation of exchange and stronger SIE effects, where the magnitude of the SIE energy is primarily due to the contribution of the core orbitals. The GGA exchange hole is more compact, which leads to an exaggeration of exchange in the bond and the nonbonding region and negative SIE contributions. Partitioning of the SIE into intra-/interelectronic and individual orbital contributions makes it possible to test the performance of a given exchange functional in different regions of the molecule. It is shown that Hartree–Fock exchange always covers some long-range effects via interelectronic exchange while self-interaction-corrected DFT is lacking these effects.

Keywords: Self-interaction error – Dynamic electron correlation – GGA exchange hole – LDA exchange hole

1 Introduction

The performance of Kohn–Sham (KS) density functional theory (DFT) [1, 2] depends on the electron correlation effects covered by the approximate exchange–correlation

(XC) functionals currently in use [3]. XC functionals have been derived utilizing the homogeneous (local density approximation, LDA [4]) or weakly inhomogeneous (generalized gradient approximation, GGA [5]) electron gas as a suitable starting point. The general understanding is that the exchange functional reasonably describes the exchange interactions of the electrons, while the correlation functional accounts for the short-range (dynamic) Coulomb correlation effects [1, 2, 3, 4, 5]. Long-range (nondynamic or static) correlation effects needed for systems with multireference character (e.g. in the case of stretched bonds) are considered not to be covered by approximate XC functionals. Of course, if the correct XC functional were known, both short- and long-range correlation would be correctly accounted for.

Nevertheless, KS DFT is also capable of reasonably describing multireference systems in those cases where Hartree–Fock (HF) seriously fails. This raises the question how multireference effects (long-range correlation) are mimicked by KS DFT. A number of authors [6, 7, 8, 9, 10, 11, 12, 13, 14, 15] have pointed out that the DFT exchange energy contains long-range correlation effects: While the exact exchange hole is generally long-ranged, encompassing larger regions of the molecule, the DFT model exchange hole, in contrast, is centered at the reference point \mathbf{r} in the case of the LDA and close to it in the case of the GGA. The difference between the true (delocalized) exchange hole and the (localized) model DFT exchange hole is expected to mimic long-range correlation effects [6, 7, 8, 9, 10, 11, 12, 13, 14, 15].

In recent work [11, 12, 13, 14], we showed that the one-particle density is a sensitive probe for the way a quantum chemical method incorporates electron correlation. For this purpose, the density distribution, $\rho(\mathbf{r})$, of a molecule obtained by DFT with a given XC functional is compared with the corresponding density calculated with a wave-function-based method, which is known to cover well-defined electron correlation effects.

The analysis of DFT exchange-only calculations [13,14,15] revealed that both LDA and GGA exchange functionals account for long-range Coulomb correlation

Correspondence to: E. Kraka
e-mail: kraka@theoc.gn.se

effects. Furthermore, it could be demonstrated [12, 13, 14, 15] that this is related to the self-interaction error (SIE) [16,17,18,19] of the approximate DFT exchange functionals. Through analysis of the SIE with the help of the exchange hole, it becomes obvious that the SIE mimics the separation of electrons in a way typical of long-range Coulomb correlation [14, 15]. Consequently, any self-interaction-corrected (SIC) DFT leads to density distributions similar to HF densities, i.e. SIC-DFT exchange does not mimic any long-range Coulomb correlation [14, 15].

A distinction between short-range and long-range correlation effects is best carried out with the help of the pair density distribution or the related XC hole. A complete description of the pair density or, alternatively, the XC hole would require an investigation of the pair density or the hole function for an infinite number of reference points; however, in practice it is sufficient to study the features of the XC hole for a small number of representative reference points, which can be associated with core, bonding, and nonbonding electrons [14].

In a recent publication [14], we discussed the relationship between LDA, SIC-LDA, and HF exchange by comparing the corresponding exchange holes. The current work extends these investigations to the more interesting GGA exchange functionals by considering the following questions:

1. How does the GGA exchange hole differ from the LDA exchange hole and how do these differences result from differences in the corresponding SIC-DFT and SIE holes?
2. How do the SIC-GGA and the SIC-LDA exchange holes reflect the properties of the HF exchange hole and how do they differ from the latter?
3. What correlation effects are mimicked by the SIE-hole? Are these just long-range effects or also short-range (dynamic) correlation effects?
4. How do intra- and interelectronic exchange influence the structure of the exchange hole? What is their role in the case of the SIC-DFT exchange hole and how do they relate to the SIE and the correlation effects simulated by the SIE?
5. Why is the energy associated with the SIE always large and positive for LDA but small and mostly negative for GGA functionals? Can these trends be related to individual orbital contributions? What is the role of core and the valence electrons in this respect?
6. Can one relate the stability of a given restricted DFT method to the structure of the exchange hole it produces?
7. Handy and Cohen [10] argued that exchange always comprises long-range (nondynamic) electron correlation effects, i.e. even in the case of HF exchange. Can this statement be supported by the analysis of the HF exchange hole?

When answering these questions one has to consider the fact that the model XC holes used in DFT calculations were derived in a way to compensate specific errors as much as possible by simple averaging techniques. As has been pointed out by a number of authors [20, 21, 22], KS

calculations benefit from the fact that, despite an often rather poor pointwise approximation to the exact XC holes, the errors of the model exchange holes largely cancel out in the calculation of the total XC energy owing to angular and system averaging. Consequently, system-averaged XC holes have been discussed extensively in the literature [9]. In the current paper, in contrast, we investigate the exchange hole point by point. This viewpoint is of interest for two reasons. On the one hand, local quantities such as the density distribution will be affected by inaccuracies of the local XC hole. On the other hand, many features of the DFT hole (e.g. their capability of mimicking nondynamic correlation effects) can be understood only from this local viewpoint.

The results of this work are presented by first summarizing some well-known properties of exchange holes (Sect. 2). Then, equations and formulas for the SIC-DFT and SIE exchange hole are derived in Sect. 3. The impact of the SIE on the structure of the LDA and GGA exchange hole is discussed in Sect. 4, while an account on the Coulomb correlation effects introduced by a DFT exchange functional is given in Sect. 5.

2 The exchange hole in HF and DFT

The properties of HF and DFT exchange holes have been repeatedly and extensively investigated Ref. [3a] and, therefore, we will summarize here only some well-known facts.

The correlated movements of the electrons of an atom or molecule can be described with the help of the XC hole, which indicates how an electron at the reference position \mathbf{r} influences the probability of finding another electron at the position $\mathbf{r} + \mathbf{R}$. The XC hole, h_{XC} is defined by Eq. (1):

$$P(\mathbf{r}, \mathbf{r} + \mathbf{R}) = \varrho(\mathbf{r})[\varrho(\mathbf{r} + \mathbf{R}) + h_{XC}(\mathbf{r}, \mathbf{r} + \mathbf{R})] , \quad (1)$$

where $P(\mathbf{r}, \mathbf{r} + \mathbf{R})$ is the pair density distribution. h_{XC} can be divided into two parts, namely the exchange hole, h_X , and the correlation hole, h_C , which are related to exchange and Coulomb correlation, respectively. The pair density is symmetric in its two arguments, hence the exchange hole (as well as the correlation hole) must obey the relation

$$\varrho(\mathbf{r})h_X(\mathbf{r}, \mathbf{r} + \mathbf{R}) = \varrho(\mathbf{r} + \mathbf{R})h_X(\mathbf{r} + \mathbf{R}, \mathbf{r}) . \quad (2)$$

2.1 HF exchange hole

The HF exchange hole for a closed-shell system is given by Eq. (3) [3a]:

$$h_X^{\text{HF}}(\mathbf{r}, \mathbf{r} + \mathbf{R}) = -\frac{2}{\varrho(\mathbf{r})} \sum_{i,i'} \varphi_i(\mathbf{r})\varphi_i(\mathbf{r} + \mathbf{R}) \times \varphi_{i'}(\mathbf{r})\varphi_{i'}(\mathbf{r} + \mathbf{R}) , \quad (3)$$

where the factor of 2 accounts for the spin summation. As Eq. (3) shows, exchange decreases the probability of finding two equal-spin electrons at the same position to

zero. However, it does not affect the corresponding probability for opposite-spin electrons.

From Eq. (3), the following relations follow:

$$h_X^{\text{HF}}(\mathbf{r}, \mathbf{r}) = -\frac{1}{2}q(\mathbf{r}) , \quad (4a)$$

$$h_X^{\text{HF}}(\mathbf{r}, \mathbf{r} + \mathbf{R}) \leq 0 , \quad (4b)$$

$$\int d^3R h_X^{\text{HF}}(\mathbf{r}, \mathbf{r} + \mathbf{R}) = -1 . \quad (4c)$$

According to Eq. (4a), the structure of the exchange hole is related to the HF density distribution and it is negative (or zero) everywhere. The exchange hole is deeper (the corresponding exchange energy density more negative), the more strongly h_X is concentrated around the reference electron (see Eq. 4b, c).

The exchange hole takes care of the self-interaction problem by annihilating the self-repulsion energy of electron pairs, which consists of twice the same electron, by an equal amount of self-exchange energy. In addition, h_X describes the Fermi correlation between different electrons, i.e. it accounts for the antisymmetry of the total wave function. Consequently, h_X can be split into two parts: a contribution $h_X^{\text{HF,intra}}$ accounting for the self-exchange, and a contribution $h_X^{\text{HF,inter}}$ that describes the Fermi correlation.

$$h_X^{\text{HF,intra}}(\mathbf{r}, \mathbf{r} + \mathbf{R}) = -2 \sum_i \frac{q_i(\mathbf{r})}{q(\mathbf{r})} q_i(\mathbf{r} + \mathbf{R}) , \quad (5a)$$

$$q_i(\mathbf{r}) = [\varphi_i(\mathbf{r})]^2 , \quad (5b)$$

$$h_X^{\text{HF,inter}}(\mathbf{r}, \mathbf{r} + \mathbf{R}) = h_X^{\text{HF}}(\mathbf{r}, \mathbf{r} + \mathbf{R}) - h_X^{\text{HF,intra}}(\mathbf{r}, \mathbf{r} + \mathbf{R}) . \quad (5c)$$

For $h_X^{\text{HF,intra}}$, Eq. (4b) and (4c) holds, i.e. intraelectronic HF exchange hole is always nonpositive and integrates to -1 . This implies that the electron pair consisting of twice the reference electron is discarded from the pair density. In contrast, $h_X^{\text{HF,inter}}$ integrates to zero for any position \mathbf{r} of the reference electron and it may assume both positive and negative values, i.e. the probability of finding the second electron is enhanced in certain regions and reduced in others. In this respect, the interelectronic exchange hole resembles the correlation hole, which has the same properties.

The components $h_X^{\text{HF,inter}}$ and $h_X^{\text{HF,intra}}$ depend on the choice of orbitals (canonical, localized, etc.), while their sum h_X^{HF} is invariant to orbital rotations. In molecules with only a few electrons of the same spin, the self-exchange dominates the features of the exchange hole and in particular the exchange energy. The self-exchange part of the exchange energy is generally more negative for localized than for delocalized (canonical) orbitals. It is convenient to use localized orbitals for the discussion of intra- and interelectronic exchange because in this way the structure of $h_X^{\text{HF,intra}}$ dominates the structure of h_X^{HF} , thus simplifying the discussion.

For the case of a two-electron system with coupled electron spins (H_2 , etc.), Eq. (5a), (5b) and (5c) take the form of Eq. (6a) and (6b):

$$h_X^{\text{HF,intra}}(\mathbf{r}, \mathbf{r} + \mathbf{R}) = h_X^{\text{HF}}(\mathbf{r}, \mathbf{r} + \mathbf{R}) = -\frac{1}{2}q(\mathbf{r} + \mathbf{R}) , \quad (6a)$$

$$h_X^{\text{HF,inter}}(\mathbf{r}, \mathbf{r} + \mathbf{R}) = 0 , \quad (6b)$$

i.e. the exchange hole describes only the self-exchange of the electrons and the corresponding exchange hole is static, i.e. it is independent of the position of the reference electron.

2.2 LDA exchange hole

DFT approximates the exact exchange hole by model exchange holes. The simplest approximation is given by the LDA model hole [4]:

$$h_X^{\text{LDA}}(\mathbf{r}, \mathbf{r} + \mathbf{R}) = -\frac{1}{2}q(\mathbf{r})J(2k_F R) , \quad (7a)$$

$$J(z) = -\frac{72}{z^6}[4 + z^2 - (4 - z^2)\cos z - 4z\sin z] , \quad (7b)$$

where $z = 2k_F R$ and $k_F = [3\pi^2 q(\mathbf{r})]^{1/3}$. The LDA exchange hole is spherically symmetric. Its minimum, given by $-q(\mathbf{r})/2$, i.e. the negative density for one of the spin orientations, is always at the position of the reference electron, but apart from this the LDA exchange hole does not reflect any features of the electron density. The LDA density hole obeys Eq. (4a), (4b), and (4c) [22] and, therefore, it becomes more compact as the density at position \mathbf{r} increases.

2.3 Gradient expansion approximation and GGA exchange hole

A more elaborate approximation for the exchange hole is obtained by considering not only the local density but also its gradient. In the original gradient expansion approximation (GEA) [23], the homogeneous electron gas as a model system is replaced by a weakly inhomogeneous one, and the exchange hole is represented as a Taylor expansion in powers of the density gradient at the reference point. Owing to the uniform scaling relation for the exchange energy [24], this actually amounts to an expansion in powers of the reduced density gradient $\mathbf{s}(\mathbf{r})$. The GEA exchange hole is represented by Eq. (8a), (8b), (8c), (8d), and (8e) [25, 26]:

$$h_X^{\text{GEA}}(\mathbf{r}, \mathbf{r} + \mathbf{R}) = -\frac{1}{2}q(\mathbf{r})[J(z) + L(z)\hat{\mathbf{R}} \cdot \mathbf{s}(\mathbf{r}) - M(z)(\hat{\mathbf{R}} \cdot \mathbf{s}(\mathbf{r}))^2 - N(z)s^2(\mathbf{r})] , \quad (8a)$$

$$\mathbf{s}(\mathbf{r}) = \nabla q(\mathbf{r}) / (2k_F(\mathbf{r})q(\mathbf{r})) \quad (8b)$$

$$L(z) = 12[2 - 2\cos z - z\sin z]/z^3 , \quad (8c)$$

$$M(z) = [-z\cos z + \sin z]/3z , \quad (8d)$$

$$N(z) = [8 - (8 - 4z^2)\cos z - (8z - z^3)\sin z]/z^4 . \quad (8e)$$

The GEA is not always negative and thus violates Eq. (4c) [23]. The resulting GEA exchange potential diverges for large values of $\mathbf{s}(\mathbf{r})$; it becomes infinite far away from the center of a finite electron system. A better description is obtained by the GGA model hole, for which Eq. (4b) and (4c) are restored by cutoff procedures [26]: in all regions, where the GEA exchange hole is positive, its value is reduced to zero: the exchange hole obtained in step 1 is set to zero outside a sphere around the reference point, the radius of which is determined in such a way that the resulting exchange hole obeys Eq. (4c).

In this way, the GGA exchange hole adopts the form in Eq. (9):

$$h_X^{\text{GGA}}(\mathbf{r}, \mathbf{r} + \mathbf{R}) = h_X^{\text{GEA}}(\mathbf{r}, \mathbf{r} + \mathbf{R}) \Theta[-h_X^{\text{GEA}}(\mathbf{r}, \mathbf{r} + \mathbf{R})] \times \Theta[R_{\text{cut}}(\mathbf{r}) - |\mathbf{R}|] , \quad (9)$$

where $R_{\text{cut}}(\mathbf{r})$ is determined by

$$\int_{|\mathbf{R}| < R_{\text{cut}}(\mathbf{r})} d^3R h_X^{\text{GGA}}(\mathbf{r}, \mathbf{r} + \mathbf{R}) \Theta[h_X^{\text{GGA}}(\mathbf{r}, \mathbf{r} + \mathbf{R})] = -1 \quad (10)$$

and Θ represents the cutoff function. The cutoff of the GGA exchange hole restores not only the correct normalization of the exchange hole but also discards the long-range tails of the GEA exchange hole, which are an artifact of the Taylor expansion.

The GGA exchange hole has the same value and gradient as the exact one at \mathbf{r} , and its minimum does not coincide with the reference position unless $\mathbf{s}(\mathbf{r}) = 0$. Because of its construction it reflects features of the exact exchange hole close to \mathbf{r} more accurately than the LDA exchange hole does; however, for positions farther away from \mathbf{r} , the deviation of the GGA exchange hole from the exact one may even be larger than for the LDA exchange hole.

In DFT calculations, the exchange energy density resulting from the model exchange hole is needed in analytical form. A number of parameterizations have been given for the energy density resulting from the GGA exchange hole of Eq. (9) [5, 26, 27, 28]. In this work, we use the Perdew–Wang 91 (PW91) exchange functional [27]; however, conclusions drawn for PW91 exchange are equally valid for other GGA exchange functionals, such as the Becke 88 (B88) functional [5].

DFT model exchange holes cannot be associated with any distribution of electron pairs as they may yield negative values for the pair density in certain regions. Moreover, they do not lead to a symmetric pair density, i.e. they violate Eq. (2). This means that care has to be taken when the impact of DFT exchange on the one-particle density is discussed.

3 SIE and SIC in DFT

For the ground-state density of a system containing only one α -spin electron, i.e. $\int d^3r \varrho_\alpha(\mathbf{r}) = 1$, and $\varrho_\beta(\mathbf{r}) = 0$, the correct exchange and correlation functional must obey the relations

$$E_J[\varrho] + E_X[\varrho_\alpha, 0] = 0 , \quad (11)$$

$$E_C[\varrho_\alpha, 0] = 0 . \quad (12)$$

This simply means that the exchange energy cancels the nonphysical self-repulsion energy of the electron and that there is no Coulomb correlation of an electron with itself. The approximate XC functionals, which are nowadays used in DFT calculations, generally violate either Eq. (11), Eq. (12), or both and, therefore, contain an incorrect electron self-interaction unless the XC functionals include SICs.

In this work, we apply the SIC-DFT approach by Perdew and Zunger [16], which corrects the SIE in the conventional DFT XC functionals orbital by orbital:

$$\begin{aligned} E_X^{\text{correct}} &= E_X^{\text{approx}}[\varrho_\alpha, \varrho_\beta] \\ &\quad - \sum_{\sigma=\alpha,\beta} \sum_i^{N_\sigma} (E_J[\varrho_{i\sigma}] + E_X^{\text{approx}}[\varrho_{i\sigma}, 0]) \\ &= E_X^{\text{approx}}[\varrho_\alpha, \varrho_\beta] - E_X^{\text{SIC}} , \end{aligned} \quad (13)$$

$$\begin{aligned} E_C^{\text{correct}} &= E_C^{\text{approx}}[\varrho_\alpha, \varrho_\beta] - \sum_{\sigma=\alpha,\beta} \sum_i^{N_\sigma} E_C^{\text{approx}}[\varrho_{i\sigma}, 0] \\ &= E_C^{\text{approx}}[\varrho_\alpha, \varrho_\beta] - E_C^{\text{SIC}} , \end{aligned} \quad (14)$$

thus yielding the following expression for the total electronic energy:

$$\begin{aligned} E^{\text{SIC-DFT}}[\varrho] &= E_T[\varrho] + E_V[\varrho] + E_J[\varrho] + E_X[\varrho] \\ &\quad - E_X^{\text{SIC}}[\varrho] + E_C[\varrho] - E_C^{\text{SIC}}[\varrho] , \end{aligned} \quad (15)$$

where E_T and E_V denote the kinetic energy of noninteracting electrons and the potential energy (nucleus–electron attraction), respectively. The corresponding KS equations are established by requiring that the energy functional (Eq. 15) should be minimal for a set of orthonormal KS orbitals. In contrast to conventional KS-DFT, the functional (Eq. 15) is not invariant with respect to rotations between the occupied orbitals, i.e. by solving the KS equations one has to make the functional stationary both with respect to rotations between occupied and virtual orbitals and with respect to rotations between occupied orbitals [17]. The theory and implementation of a self-consistent SIC-DFT procedure (SCF-SIC-DFT) are described in Ref. [29].

An alternative to SCF-SIC-DFT is perturbative SIC-DFT, where after a conventional KS-DFT calculation, the SICs are computed in one step from the KS orbitals. Perturbational SIC-DFT requires a careful choice of the appropriate KS orbitals. The SIC-DFT equations require the use of localized orbitals [17] and, therefore, the KS orbitals are localized by a Foster–Boys localization procedure [30]. In SIC-DFT, approximate (LDA or GGA) self-exchange is replaced, orbital by orbital, by the exact self-exchange:

$$\begin{aligned} h_X^{\text{SIC-DFT}}(\mathbf{r}, \mathbf{r} + \mathbf{R}) &= h_X^{\text{DFT}}(\mathbf{r}, \mathbf{r} + \mathbf{R}) \\ &\quad - \sum_i \frac{\varrho_i(\mathbf{r})}{\varrho(\mathbf{r})} \left[h_{X,i}^{\text{DFT}}(\mathbf{r}, \mathbf{r} + \mathbf{R}) \right. \\ &\quad \left. + 2\varrho_i(\mathbf{r} + \mathbf{R}) \right] , \end{aligned} \quad (16)$$

where $h_{X,i}^{\text{DFT}}$ denotes an orbital exchange hole evaluated with the density $2q_i$. The SIC-DFT exchange hole fulfills Eq. (4a) and (4c), but not necessarily Eq. (4b). The SIE part of the DFT (LDA or GGA) exchange hole (henceforth called SIE exchange hole) is then given by

$$\begin{aligned} h_X^{\text{SIE}}(\mathbf{r}, \mathbf{r} + \mathbf{R}) &= h_X^{\text{DFT}}(\mathbf{r}, \mathbf{r} + \mathbf{R}) \\ &\quad - h_X^{\text{SIC-DFT}}(\mathbf{r}, \mathbf{r} + \mathbf{R}) \\ &= \sum_i \frac{q_i(\mathbf{r})}{q(\mathbf{r})} \left[h_{X,i}^{\text{DFT}}(\mathbf{r}, \mathbf{r} + \mathbf{R}) \right. \\ &\quad \left. + 2q_i(\mathbf{r} + \mathbf{R}) \right]. \end{aligned} \quad (17)$$

The SIE exchange hole integrates to zero for a given reference position and can be both positive and negative.

SIC-DFT and SIE energies were calculated for a number of first row diatomic molecules by employing one LDA and two GGA XC functionals: SVWN5 (LDA: Slater exchange [4] is combined with the Vosko, Wilk, and Nusair correlation functional V [31]); BLYP (GGA: B88 exchange [5] is combined with the Lee, Yang, and Parr [32] correlation functional); and PW91PW91 (GGA: the XC functional of Perdew and Wang [27] is used). The three functionals were used both in exchange-only and normal (including both exchange and correlation) calculations.

The calculated SIE energies were analyzed by comparing the structure of the HF, LDA (Slater exchange), GGA (PW91 exchange), SIC-DFT (SIC-S and SIC-PW91), and SIE (SIE-S and SIE-PW91) exchange holes. Different X functionals yield different densities for a given system. Correspondingly, the resulting exchange holes will differ from each other owing to differences in the one-particle density and owing to the different way the different functionals describe exchange. In the current work, differences due to the former reason are suppressed by using HF orbitals for both HF and DFT descriptions of the exchange hole.

The results for H_2 and F_2 are discussed in detail, because they are representative for other diatomic molecules investigated in this work. All the calculations were carried out with Dunning's cc-pVTZ basis [33] at experimental geometries, i.e. $d(\text{H} - \text{H}) = 0.742 \text{ \AA}$ for H_2 ($^1\Sigma_g^+$), $d(\text{F} - \text{F}) = 1.412 \text{ \AA}$ for F_2 ($^1\Sigma_g^+$) [34]. The calculations were carried out with the program package Cologne 2001 [35].

4 The impact of the SIE on the structure of LDA and GGA exchange holes

Because of the fact that for H_2 ($^1\Sigma_g^+$) only intraelectronic exchange, but no interelectronic exchange exists, it is a useful starting point for studying properties of DFT exchange holes. In Fig. 1, HF, LDA, and GGA exchange holes are shown for two positions \mathbf{r} of the reference electron, namely for the reference electron being located in the bond region closer to nucleus H1 ($\mathbf{r} = \text{P1}$, Fig. 1a), separated from H1 by the distance $d/4$, and for the reference electron being located in the nonbonding region of H1 ($\mathbf{r} = \text{P2}$, Fig. 1b), again separated from H1 by $d/4$. Actually, the situation in

which the reference electron is located at the bond midpoint may also be considered. However, in this situation LDA and GGA exchange holes do not differ from each other (the reduced density gradient \mathbf{s} vanishes) and conclusions drawn for the LDA exchange hole at P1 are equally valid [14]. In this publication, we are mainly interested in the corrections caused by the GGA functional and, therefore, we investigate those locations \mathbf{r} where the reduced density gradient is large, i.e. positions such as P1 and P2.

According to Eq. (6a) and (6b), the HF exchange hole is static and equates to the negative density per spin direction, i.e. the negative density of one σ_g electron. The HF exchange hole is delocalized over the whole molecule and reflects features of the electronic structure. As the same density is used for HF and DFT, the SIC-DFT holes (LDA and GGA) are identical to the HF exchange hole for H_2 (Fig. 1). The SIE hole for the H_2 molecule is simply given by the difference between DFT and HF exchange holes.

Irrespective of the position of the reference electron, the LDA and GGA exchange holes are always more localized than the HF exchange hole. While the LDA hole is completely insensitive to the electronic structure, the GGA exchange hole reproduces to some extent the local minimum of the HF exchange hole at the H1 atom (Fig. 1), in line with the fact that the GGA more accurately reflects features of the exchange hole close to the reference point than LDA does. This is also reflected by the SIE part of the DFT exchange holes. At H1, the SIE part obtained with the GGA functional is smaller than that obtained with the LDA functional (Fig. 1a). However, both functionals drastically exaggerate the probability of finding the second electron at H2 although the error is larger for the GGA than the LDA functional (Fig. 1a). As pointed out in Ref. [14], the SIE mimics in this way long-range left-right electron correlation for the bonding electron pair of H_2 ($^1\Sigma_g^+$) where this effect is a result of the nonphysical self-interaction of each electron rather than the interaction between the two electrons.

For the reference electron being located at P2 in the nonbonding region similar effects are observed as for situation P1 (Fig. 1b). However, deviations between the LDA and the GGA exchange hole are now much larger as are the differences in the corresponding SIE holes. This is due to the fact that the reduced gradient \mathbf{s} is larger at P2 (at P2 the density is smaller and the density gradient larger than at P1), which gives rise to larger gradient corrections. The LDA exchange hole is shallower and more diffuse because the density at P2 is lower than at P1. In contrast, the GGA exchange holes for $\mathbf{r} = \text{P1}$ and P2 are similarly deep and have approximately the same spatial extent, with the one for P2 being only somewhat more diffuse. The movement of the reference electron from P1 to P2 leads to less distinct changes in both the shape and the position of the minimum of the GGA exchange hole than in case of the LDA exchange hole, i.e. the GGA exchange hole reproduces the static character of the HF exchange hole to some extent, while the LDA exchange hole is clearly nonstatic. Of course, the GGA exchange hole is no

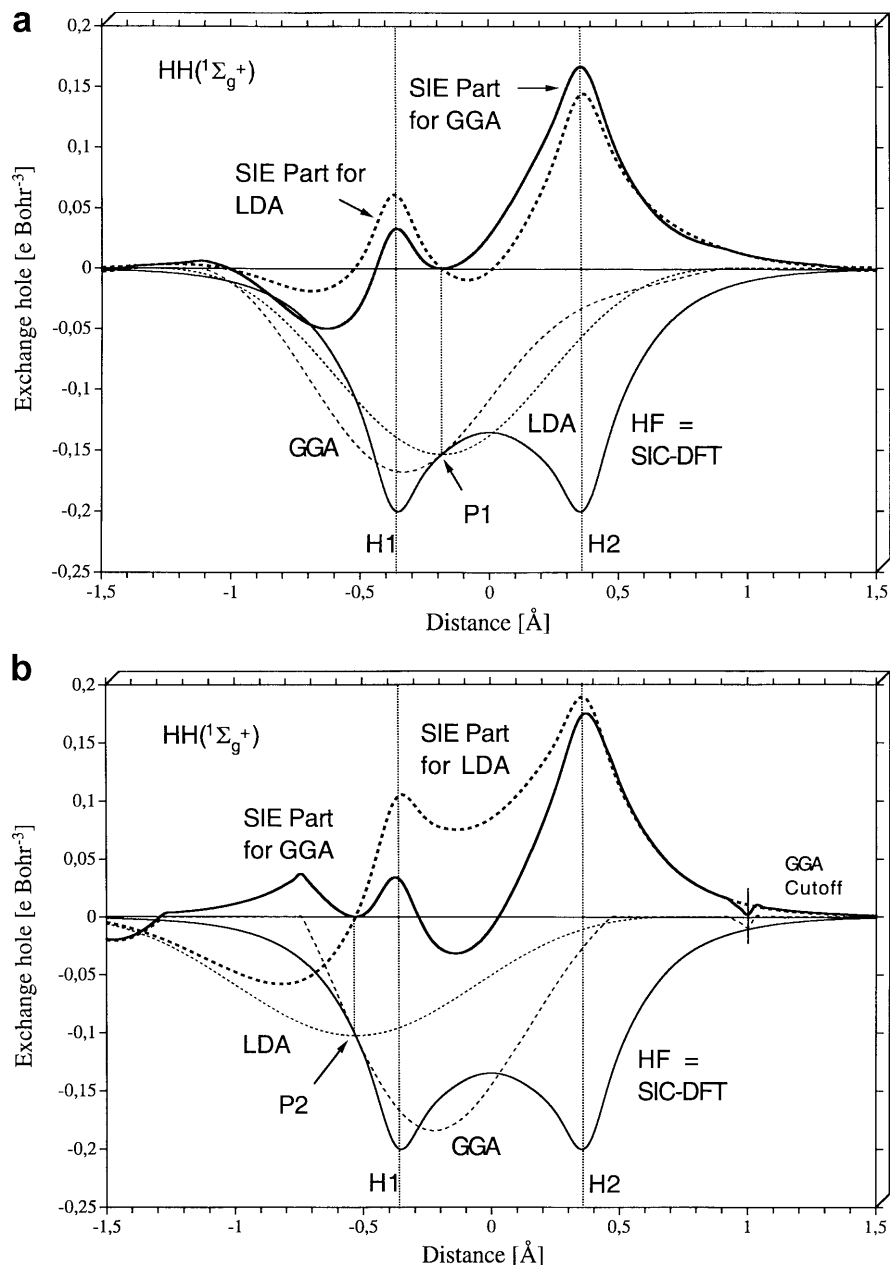


Fig. 1. Graphical representation of the exchange hole calculated for H_2 ($^1\Sigma_g^+$) along the bond axis at the Hartree-Fock (HF) (solid line), local density approximation (LDA) (short-dashed line) and, generalized gradient approximation (GGA) (long-dashed line) levels of theory for the reference electron being **a** at position P1 and **b** at position P2. The self-interaction-error (SIE) parts of the GGA and LDA hole are indicated in bold and bold-dashed print, respectively. All calculations with a cc-pVTZ basis set at the experimental H-H distance

longer static, whilst the reference electron is moved across the bond center; in this case, the center of gravity for the GGA exchange hole moves from the left to the right H atom.

The SIE of the GGA functional again mimics stronger left-right correlation effects than the SIE-LDA. The SIE holes also differ in the nonbonding region of H1 where SIE-GGA shows a small peak, which is due to the cutoff in the GGA exchange hole and, accordingly, has no counterpart in the LDA exchange hole. The GGA mimics in this way some short-range electron correlation since there is an enhanced probability of finding the second electron to the left and to the right of the position of the reference electron at P2. The LDA mimics short-range correlation in so far as it moves the density of the second electron from the nonbonding region to the position of H1 and in the bonding region. This effect is

related to the observation that the LDA severely overestimates the bond density and, by this, also the bond strength.

Energetically, both long-range and short-range effects have a strong impact on the calculated exchange energy of H_2 . The diffuse character of the LDA hole in particular in the low-density regions leads to a serious underestimation of exchange and, therefore, to a large, positive SIE, i.e. Coulomb self-repulsion dominates the LDA-SIE. Since the GGA exchange hole is less diffuse, the SIE energy is smaller but still positive. (Generally, the exchange energy becomes more negative as the exchange hole becomes more localized.) However, the most important conclusion directly drawn from Fig. 1 is that both the SIE-GGA and the SIE-LDA mimic long-range left-right correlation effects irrespective of the position of the reference electron.

In most diatomic molecules both intra- and inter-electronic exchange play a role. In this case, both intra- and interelectronic HF exchange holes as well as the total HF exchange hole depend on the position of the reference electron, i.e. none of the HF exchange holes is any longer static when a multielectron system is considered. Both localized (reference electron at or close to the nucleus), slightly delocalized (P in the lone pair region), and strongly delocalized HF exchange holes (P in the bond region) can be found, while in all these cases the DFT exchange holes are localized (LDA at P; GGA at a point off P). In Figs. 2, 3, 4, 5, 6, 7, HF and DFT exchange holes are shown for positions P1 and P2 of the reference electron (Figs. 2, 4); the decompositions of the

exchange hole into orbital contributions (Fig. 3 for P1, Fig. 7 for P2) or intra- and interelectronic part (Fig. 5 for P1, Fig. 6 for P2) are also shown. The molecular space is partitioned along the molecular axis into seven regions to facilitate the discussion: A and B correspond to the valence regions of F1 and F2, C to the bond region, D and E to the nonbonded regions of F1 and F2, and F and G to the tail regions of F1 and F2. The calculated SIE energies are analyzed in Tables 1 and 2.

The structure of the HF exchange hole shown in Figs. 2 and 3 can be analyzed in terms of intra- and interelectronic contributions (Figs. 5, 6), which in turn can be related to the form of the occupied orbitals. In the case of F_2 (${}^1\Sigma_g^+$), Foster–Boys localization of the occupied

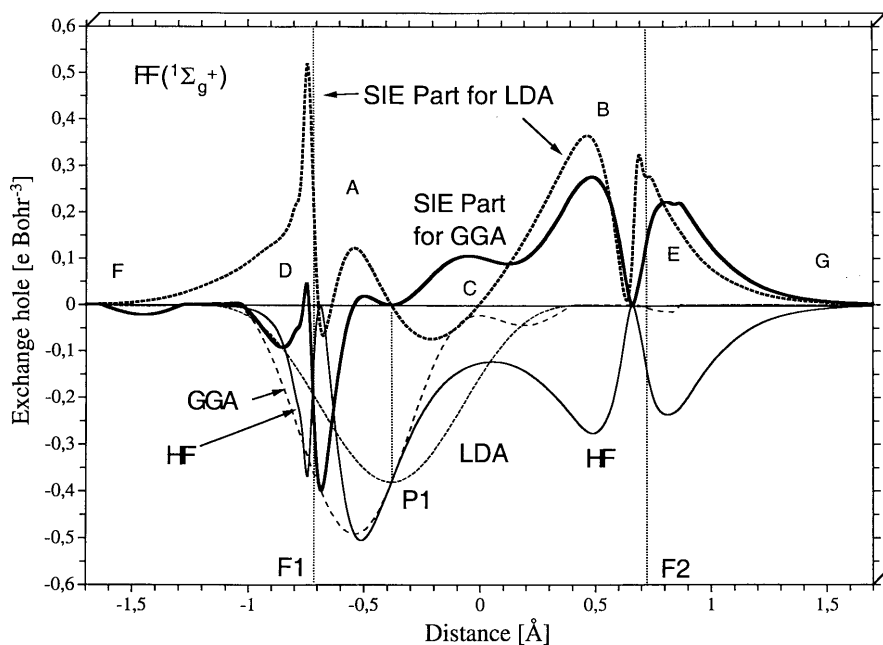


Fig. 2. Graphical representation of the exchange hole calculated for F_2 (${}^1\Sigma_g^+$) along the bond axis at the HF (solid line), LDA (short-dashed line), and GGA (long-dashed line) levels of theory for the reference electron being at position P1. The SIE parts of the GGA and LDA hole are indicated in bold and bold-dashed print, respectively. All calculations with a cc-pVTZ basis set at the experimental geometry

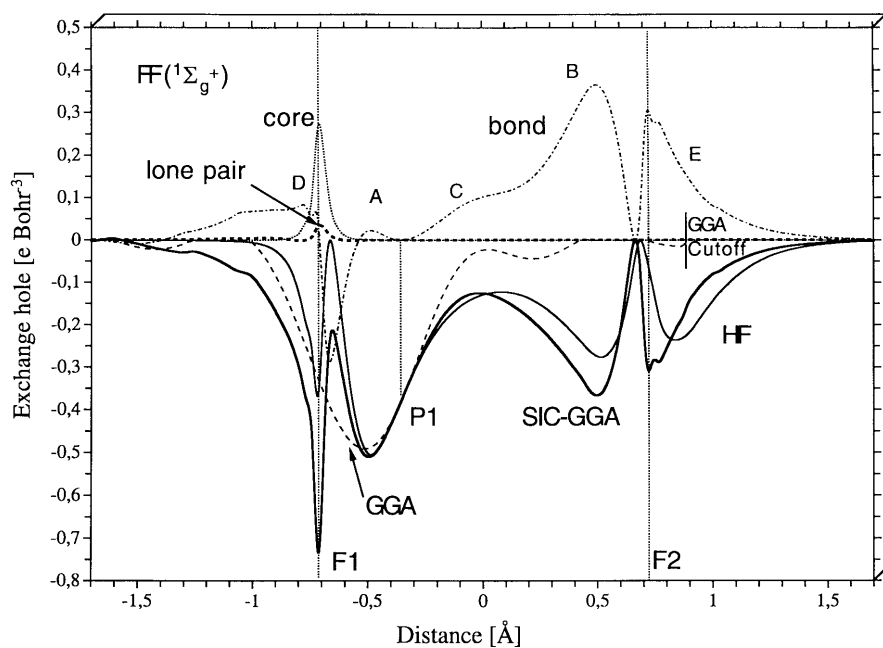


Fig. 3. Graphical representation of the exchange hole calculated for F_2 (${}^1\Sigma_g^+$) along the bond axis at the HF (solid line), GGA (long-dashed line), and self-interaction-corrected (SIC)-GGA (bold line) levels of theory for the reference point being at position P1. The core, lone pair, and bond orbital contributions to the SIE of the GGA exchange functional are given by dashed lines. All calculations with a cc-pVTZ basis set at the experimental geometry

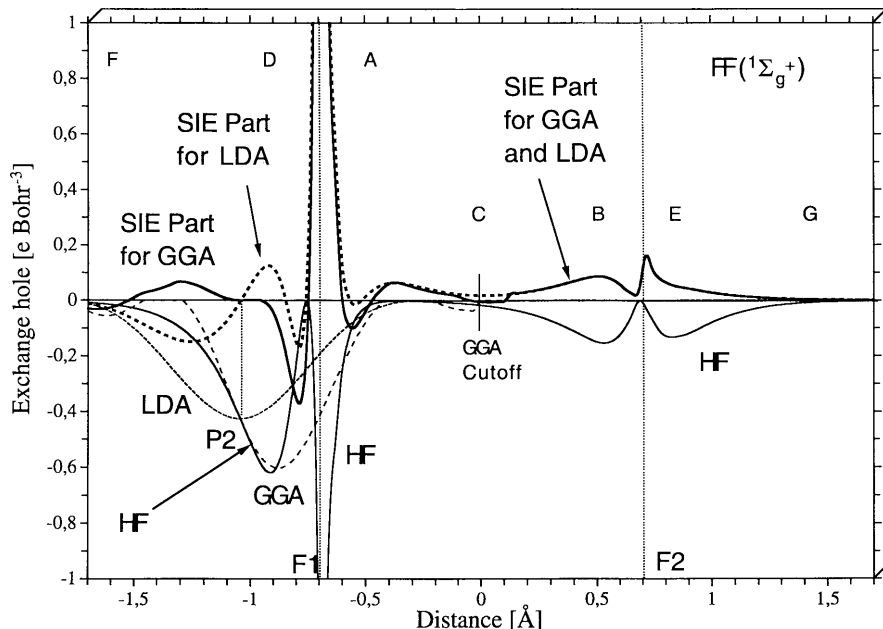


Fig. 4. Graphical representation of the exchange hole calculated for F_2 ($^1\Sigma_g^+$) along the bond axis at the HF (solid line), LDA (short-dashed line), and GGA (long-dashed line) levels of theory for the reference electron being at position P2. The SIE parts of the GGA and LDA hole are indicated in bold and bold-dashed print, respectively. All calculations with a cc-pVTZ basis set at the experimental geometry

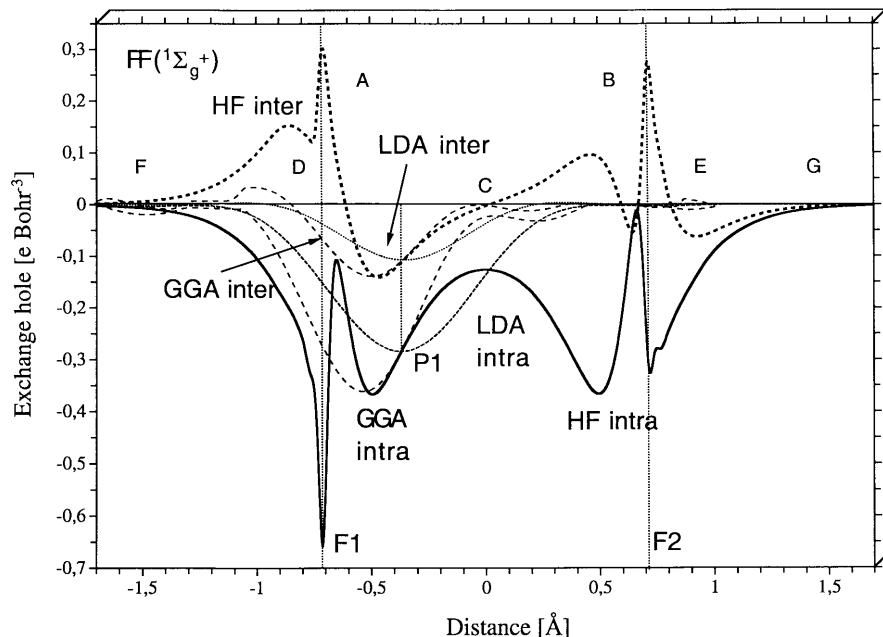


Fig. 5. Graphical representation of the intraelectronic (bold line) and interelectronic part (bold-dashed line) of the exchange hole calculated for F_2 ($^1\Sigma_g^+$) along the bond axis at the HF level. The corresponding LDA (intra: short-dashed line; inter: dotted line) and GGA (intra and inter: long-dashed lines) parts are also shown. The reference electron is at position P1. All calculations with a cc-pVTZ basis set at the experimental geometry

orbitals gives two $1s$ core orbitals, a $sp^3-sp^3-\sigma_g$ bond orbital, and six sp^3 lone pair orbitals. If the reference electron resides at the midpoint of the F–F bond, then the hole structure is dominated by the σ_g bonding orbital and reflects the negative density of the electrons in this orbital. To some extent, this is also true for the HF exchange hole when the reference electron is at P1 (Fig. 2). This one can see more clearly from its intraelectronic part (Fig. 5), which in the bond region is almost symmetrical with regard to the bond midpoint. Additional orbital contributions determine the structure of the intraelectronic HF exchange hole according to their orbital densities at P1 (cf. Eq. 5a). Both the lone pair and the core orbitals of F1 (but not of F2) possess small tails at P1. These tails, via the product $\rho_i(\mathbf{r}) \rho_i(\mathbf{r} + \mathbf{R})$ in

Eq. (5a), lead to a deepening of the intraelectronic hole at those positions where the corresponding orbital density is largest, namely at F1 (core contribution) and in region D (lone pair contributions, Fig. 5).

The interelectronic part depends on the probability of finding the reference electron at P1, i.e. in the bonding σ_g orbital, and a second electron in another orbital, which overlaps with the bonding orbital (see Eq. 3). This probability is large and positive at positions D (lone pair orbitals at F1), F1 and F2 (core orbitals), and in a part of E (lone pair orbitals at F2, see Fig. 5). The intra- and interelectronic parts together determine the structure of the HF exchange hole (Fig. 2). Note that the HF exchange hole possesses nodes close to the two nuclei, which correspond to the nodes in the bond orbital. The

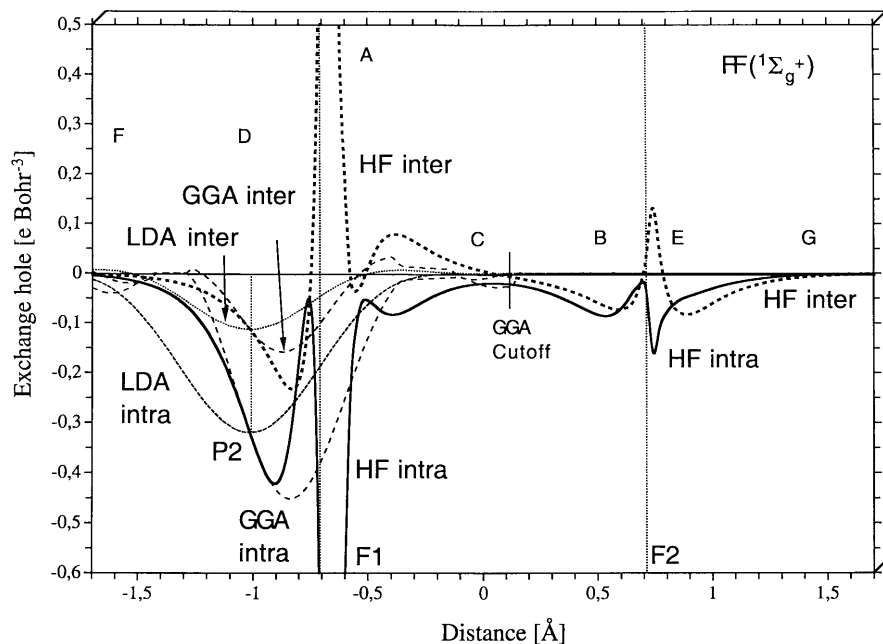


Fig. 6. Graphical representation of the intraelectronic (*bold line*) and interelectronic part (*bold-dashed line*) of the exchange hole calculated for F_2 ($^1\Sigma_g^+$) along the bond axis at the HF. The corresponding LDA (intra: *short-dashed line*; inter: *dotted line*) and GGA (intra and inter: *long-dashed lines*) parts are also shown. The reference electron is at position P2. All calculations with a cc-pVTZ basis set at the experimental geometry

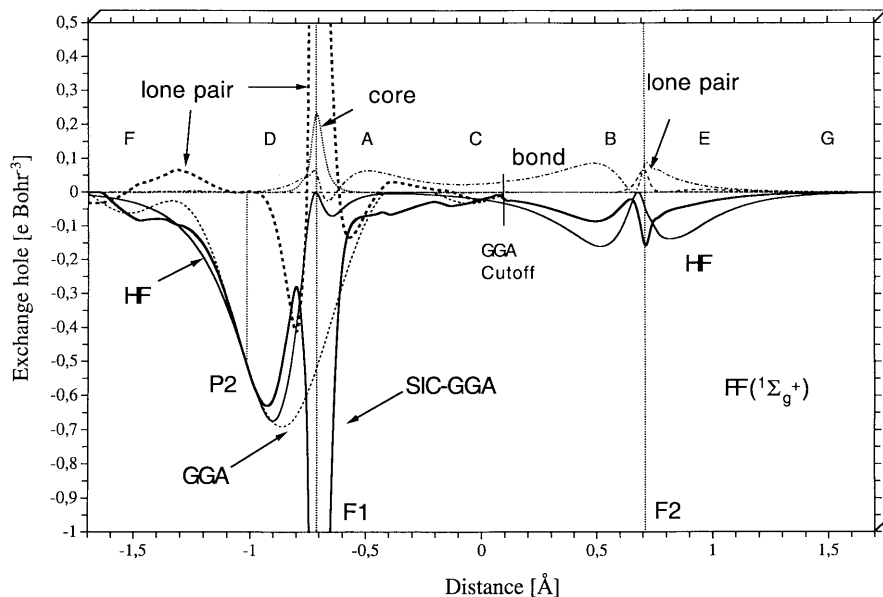


Fig. 7. Graphical representation of the exchange hole calculated for F_2 ($^1\Sigma_g^+$) along the bond axis at the HF (*solid line*), GGA (*dashed line*), and SIC-GGA (*bold line*) levels of theory for the reference point being at position P2. The core, lone pair, and bond orbital contributions to the SIE of the GGA exchange functional are given by *dashed lines*. All calculations with a cc-pVTZ basis set at the experimental geometry

latter are shifted slightly from the nuclei, typical of a bonding orbital composed of two sp^3 hybrid orbitals.

A comparison of the LDA and GGA exchange holes (Fig. 2) shows again that the latter gives a better account of the structure of the HF exchange hole close to P1. In region C, however, the GGA hole deviates more strongly from the HF exchange hole, showing in particular nonphysical tail oscillations reminiscent of the original GEA hole (Fig. 2).

The SIC-GGA hole, the HF hole (Fig. 3), and the SIC-LDA exchange hole (not shown, but see Ref. [14]) show small, but significant, differences, which reflect the three different ways of describing exchange. In the vicinity of P1, the SIC-GGA exchange hole is nearly identical to the HF exchange hole, while it is close to the

Table 1. Exchange energies, E_X , self-interaction-corrected exchange energies, $E_{\text{SIC-X}}$, and self-interaction errors, $E_{\text{X-SIE}}$ for the F_2 molecule as calculated with Hartree-Fock (HF) and different density functional theory (DFT) functionals. All calculations with Dunning's cc-pVTZ basis set [33] at the experimental geometry for the $^1\Sigma_g^+$ state of F_2 [34], i.e. $r(\text{F}-\text{F}) = 1.412\text{\AA}$. % of E_X gives the SIE in percent of the total exchange energy

	E_X	$E_{\text{SIC-X}}$	$E_{\text{X-SIE}}$	% of E_X
S only	-18.08369	-20.38508	2.30139	12.7
SVWN5	-18.12630	-20.43326	2.30696	12.7
B only	-20.06006	-19.67751	-0.38255	1.9
BLYP	-20.07834	-19.69511	-0.38323	1.9
PW91 only	-20.02280	-19.97353	-0.04927	0.2
PW91PW91	-20.04194	-19.99687	-0.04507	0.2
HF	-19.95739	-19.95739	0	0

Table 2. Orbital contributions to the SIE of different DFT exchange functionals calculated for $F_2(^1\Sigma_g^+)$. All calculations with Dunning’s cc-pVTZ basis set [33] at the experimental geometry for the $^1\Sigma_g^+$ state of F_2 [34], i.e. $r = 1.412\text{\AA}$. SIC calculated with perturbational SIC-DFT based on conventional DFT calculations. All contributions are given per orbital, i.e. not per orbital group

		$E_{X,SIE}$	$E_{X,SIE}$	$E_{X,intra}^{DFT}$	$E_{X,intra}^{HF}$	$E_{C,intra}$
SX	Core	0.76828	0.76828	-4.67697	-5.44525	
	Lone pair	0.12003	0.12003	-0.92338	-1.04341	
	F-F bond	0.04465	0.04465	-0.78429	-0.82894	
SVWN5	Core	0.67282	0.76857	-4.67896	-5.44753	-0.09575
	Lone pair	0.06546	0.12092	-0.92803	-1.04895	-0.05546
	F-F bond	-0.00823	0.04430	-0.78587	-0.83017	-0.05253
BX	Core	0.04067	0.04067	-5.43279	-5.47346	
	Lone pair	-0.05551	-0.05551	-1.10636	-1.05086	
	F-F bond	-0.13086	-0.13086	-0.95888	-0.82802	
BLYP	Core	0.04062	0.04062	-5.43280	-5.47342	
	Lone pair	-0.05556	-0.05556	-1.10865	-1.05310	
	F-F bond	-0.13116	-0.13116	-0.95971	-0.82855	
PW91X	Core	0.09320	0.09320	-5.37942	-5.47262	
	Lone pair	-0.02380	-0.02380	-1.07436	-1.05056	
	F-F bond	-0.09294	-0.09294	-0.92089	-0.82795	
PW91PW91	Core	0.07512	0.09324	-5.38005	-5.47329	-0.01812
	Lone pair	-0.03850	-0.02322	-1.07704	-1.05382	-0.01528
	F-F bond	-0.10695	-0.09214	-0.92146	-0.82932	-0.01481

intraelectronic part of the HF exchange hole at larger distances from P1. The SIC-GGA exchange hole is actually the sum of the HF intraelectronic exchange hole (note that for HF and DFT the same density was used) and a GGA interelectronic exchange hole (Fig. 5). One sees that the GGA interelectronic exchange hole agrees well with the HF interelectronic hole around P1, whereas it decays at larger distances and thus does not reflect long-range features of interelectronic exchange.

The form of the SIC-GGA exchange hole determines the SIE part of the GGA exchange hole (as does SIC-LDA for the LDA), which is given by the difference of the GGA hole and the SIC-GGA hole (Eq. 17). For the LDA, the SIE decreases the probability of finding the second electron close to the bond center, but increases the probability of finding it close to nucleus F1 or in regions D, A, B, and E (Fig. 2), thus reflecting the structure of $h_X^{HF,intra}$ in these regions. In contrast to the SIE-LDA hole, the SIE-GGA hole decreases the probability of finding the second electron at D or nucleus F1 (also A). There is an increased probability of finding it in the bond region C and in regions B and E (although smaller than given by the SIE-LDA in the latter two cases). Hence, short-range and long-range left-right correlation effects are mimicked by the SIE of the LDA and the GGA in the case of F_2 .

The SIE-GGA part of the GGA hole is largely dominated by the form of the bond orbital and the corresponding bond orbital density (Fig. 3). Hence, left-right long-range electron correlation simulated by SIE concerns preferentially the bonding electron pair when the reference electron is in the bonding region. There is a small core contribution at nucleus F1 (a large core contribution has to be weighted by a small tail contribution of the core density at P1) and vanishingly small lone pair contributions. (Note that the tails of the lone pairs are directed away from the molecular axis at an angle of about 60° .) In this connection, one has to emphasize that the orbital contributions depend on the choice of the localization procedure.

If the reference point is moved to P2, i.e. into the lone pair region D, the major part of the HF exchange hole is concentrated in the vicinity of P2 (between P2 and F1), dominated by the intraelectronic exchange of the lone pair orbitals at F1. The second major feature of the HF exchange hole is a deep, narrow depression at F1. This is caused by the three lone pair, the core, and the bond orbital contributions, which all have (larger or smaller) densities at P2 and F1. In this connection, it has to be noted that the nodal surfaces of the lone pair and the bond hybrid orbitals do not pass through the nuclei F1 and F2 but are shifted slightly into regions A and B.

The HF exchange hole is close to zero in regions A and C, but has a tail in regions B and E. The decomposition of the HF exchange hole into its inter- and intraelectronic parts (Fig. 6) reveals that the tail in regions B and E is caused by the interelectronic contribution (from the bond orbital) which is somewhat reduced by the intraelectronic one. In regions A and C, inter- and intraelectronic HF exchange cancel each other out. The former must be always negative, while the latter can become positive if one of the orbitals involved possesses a nodal surface between the position of the reference electron (P2) and the region of inspection (e.g. $(\mathbf{r} + \mathbf{R})$ in region A) as becomes clear from Eq. (3). For the bond orbital and the lone pair orbital, the overlap is negative at P2, but becomes positive in region A ($h_X^{HF,inter} > 0$, Fig. 6), changes to negative values at C ($h_X^{HF,inter} < 0$), to positive values close to F2 ($h_X^{HF,inter} > 0$), and again to negative values in region E ($h_X^{HF,inter} < 0$; the lone pair has a positive orthogonalization tail in this region).

Again, the GGA exchange hole is less sensitive to the relocation of the reference point (from P1 to P2) than the LDA exchange hole, i.e. it is more static than the LDA hole. Also, the GGA exchange hole describes better the exact exchange hole close to P2 than the LDA hole does.

The SIE-LDA hole increases the probability that the second electron is in region D, relatively close to nucleus

F1, whereas the GGA functional slightly favors a position of the second electron in the tail region F. Both the SIE-LDA and the SIE-GGA hole have a peak at nucleus F1, reflecting the fact that DFT exchange is blind to the influence of the lone pair and core electrons on the structure of the exchange hole (Fig. 7). In regions B and E, the SIE-LDA and the SIE-GGA holes are nearly identical, reflecting the structure of the intraelectronic HF exchange hole (interelectronic DFT exchange is zero in this part; Fig. 6).

Again, DFT exchange mimics some long-range left-right correlation effects where the differences between the LDA and the GGA are vanishingly small. Differences exist with regard to short-range electron correlation effects also simulated by the SIE of DFT: the SIE-LDA shifts the second electron closer to the F1 nucleus while the SIE-GGA shifts it more into the tail region F.

On the basis of the analysis of the LDA and GGA exchange holes, the orbital contributions to the SIE of the exchange energy in F_2 can be understood in detail. A number of trends are reflected by the data in Tables 1 and 2:

1. The SIE is absolutely larger and more positive for the LDA than for the GGA methods (Table 1).
2. For each of the functionals, the SIE is most positive for the core orbitals and more positive for the lone pair than for the bond orbitals (Table 2).
3. The SIE-LDA is absolutely larger than the SIE-GGA for the core and lone pair orbitals. For the bond orbitals, the SIE-LDA shows a smaller absolute deviation than the SIE-GGA (Table 2).
4. Comparing PW91 and B88, B88 gives the lowest SIE for the core orbitals, while PW91 gives a better overall agreement (Table 1).

These trends can be understood by considering two major features of the DFT exchange:

1. The LDA generates too diffuse exchange holes in regions with low density and large density gradients, which implies that the exchange energy density becomes too positive. (This can be seen in Fig. 4; stronger effects are observed for the reference electron being located in the tail regions F and G.) The asymptotic behavior of the LDA exchange energy per particle corresponds to an exponential decay, while the correct behavior is a $1/r$ decay [5,36]. The correction terms included into GGA functionals give rise to a more compact exchange hole and, thus, a more negative exchange energy. By construction, the GGA exchange energy is always more negative than the LDA exchange energy for the same density [5, 27].
2. If the HF exchange hole is strongly delocalized (depressions at two nuclei, etc.), the localized GGA exchange hole will be larger than the HF exchange hole in the vicinity of the reference electron (bond region, Fig. 2, or lone pair region, Fig. 4) although it is as deep as the HF hole. This yields an overly negative exchange energy, indicating that the error caused by Coulomb self-repulsion is overcompensated. For the core electrons, both the HF and DFT exchange holes are localized and this error does not occur.

Feature 1 immediately explains trend 1. Feature 2 explains trend 2 by considering that the core orbitals are most strongly localized and that the lone pair orbitals are constrained to a smaller space than the bond orbitals. Trend 3 is a consequence of the interplay between features 1 and 2: for the core and lone pair orbitals, feature 1 plays the dominating role for the SIE; hence the GGA gives a lower absolute SIE than LDA. For bond orbitals, in contrast, features 1 and 2 lead to a compensation of errors for the LDA, while feature 2 dominates and no error compensation takes place with a GGA description.

Trend 4 can be traced back to the way the PW91 and B88 functionals were derived. While PW91 was constructed without any reference to particular atoms or molecules [27], the construction of B88 includes a parameter fit where the B88 exchange energy was fitted to the HF exchange energy for a number of atoms, i.e. rotation-symmetrical systems [5]. This implies that B88 should be particularly accurate for compact, rotation-symmetrical density distributions, as is confirmed by trend 4. However, the small SIE for the core electrons connected with a large (negative) SIE for the bond electrons leads to a less complete cancellation of errors than in the case of PW91.

5 Exchange and Coulomb correlation as introduced by the exchange functional

The shape of the HF exchange hole, except for the case of only one electron per spin direction, depends sensitively on the location of the reference electron: If the reference electron is in the core region, the exchange hole will be dominated by the core orbitals and thus it will be short-ranged (localized) and insensitive to the large-scale electronic structure of the molecule. For the reference electron being located in the lone pair region, the HF exchange hole adopts a more complicated structure with a lone pair, a core part, and a tail region at the neighboring nucleus. The HF exchange hole becomes distinctly delocalized stretching over the (diatomic) molecule when the reference electron is located somewhere in the bond region. In both cases, the reference electron is located in the bonding or the nonbonding region (P1 and P2), and the HF exchange hole reflects features of the electronic structure of the molecule.

It is useful to partition the HF exchange hole into an intraelectronic and an interelectronic part. Even though this separation contains some arbitrariness, additional insight into the features of the exchange hole is gained, in particular, as this partitioning separates effects that have a counterpart in classical physics, viz. the cancellation of self-interactions (intraelectronic exchange), from those that are purely quantum-mechanical, viz. the Fermi exchange (interelectronic exchange).

The investigation of GGA and LDA exchange holes reveals both similarities and differences:

1. The GGA exchange hole is more sensitive to features of the electronic structure close to the reference electron than the LDA hole is. Accordingly, the

GGA reproduces the HF exchange hole more accurately in the vicinity of the reference electron. In addition, the GGA hole is more static, i.e. it changes both its shape and its center of gravity less than the LDA exchange hole does when the reference electron is moved over a small distance within a given region. For long distances from the reference point (of the order of the bond lengths), no general statement can be made, i.e. the GGA exchange hole may deviate less or more from the HF exchange hole than the LDA exchange hole.

2. If the reference electron is located within the molecule, the GGA exchange hole is compact (in contrast to the more diffuse LDA exchange hole). Neither the LDA nor the GGA exchange hole are able to reproduce features of the HF exchange hole at larger distances from the reference electron. This failure of DFT implies that both the LDA and the GGA mimic long-range left–right electron correlation effects in a molecule in an unspecified way.
3. The orbital decomposition for the SIE of the exchange energy proves that the large SIE for the LDA primarily arises from the core region as the LDA exchange hole is already too diffuse in the core region, thus yielding a too positive exchange energy density insufficient to annihilate the large positive Coulomb self-repulsion of the core electrons. The core contributions to the HF exchange hole are concentrated in space; hence, the more compact GGA hole gives a rather accurate reproduction of the HF exchange hole for the core electrons and, consequently, a small SIE in the exchange energy.
4. As regards the bond and lone pair contributions to the SIE, there is a partial compensation of errors for the LDA that is not present for the GGA. As a result, the SIE-LDA for the exchange energy may be smaller than the corresponding SIE-GGA (as found for the bonding electrons). The error compensation in the LDA case takes place in the same unspecified way as the mimicry of nondynamic electron correlation discussed in point 2.
5. The SIC-GGA exchange hole gives a rather accurate reproduction of the total HF exchange hole in the vicinity of the reference electron. At larger distances it is close to the intraelectronic part of the total HF exchange hole, similarly as the SIC-LDA exchange hole.

The investigation of H_2 , F_2 , and other diatomic molecules reveals that long-range features in the HF exchange hole occur in systems with and without interelectronic exchange, particularly if the reference electron is in the bonding region. The intraelectronic exchange is mainly responsible for the structure of the exchange hole and reflects the shape of the bonding orbital extending over the bond region and part of the nonbonding region. Although the intraelectronic part depends on the position of the reference electron and therefore is no longer static (as the intraelectronic exchange hole of H_2), changes in its form are smaller than those of the interelectronic part (Figs 5, 6). The changes of the interelectronic exchange hole stretch over the whole bonding

region (Fig. 5, regions A, B) and represent some long-range left–right correlation.

This observation reminds us of a recent statement made by Handy and Cohen [10] when considering the HF description of the dissociating H_2 molecule: exchange and nondynamic correlation cannot be separated. Even at equilibrium geometry, HF exchange accounts for long-range correlation effects as is reflected by the interelectronic part of the HF exchange hole. Hence, it is correct to say that HF exchange always contains some nondynamic (left–right) correlation provided an electron system with more than one electron pair is considered. The HF exchange hole for H_2 is purely static and does not contain any long-range nondynamic electron correlation effects.

One cannot generalize the statement that exchange always includes long-range correlation effects: the SIC-DFT hole (no matter whether the SIC-LDA or the SIC-GGA is considered) is dominated by the delocalized intraelectronic exchange hole, to which the localized interelectronic DFT part is added. If one considers that the intraelectronic exchange part does not account for significant long-range effects and the interelectronic part excludes any long-range effects since it is localized, then SIC-DFT is clearly a method (probably the only one) without any nondynamic correlation effects. This clarifies that SIC-DFT (if carried out with the HF density) should be inferior to HF as in the former case long-range correlation is absent. In this respect, there should be hardly any difference between the LDA and the GGA.

While in our previous work [14], we emphasized that the long-range correlation effects are a result of the SIE of DFT, we can detail and extend this statement in several ways:

1. The SIE does not only mimic long-range correlation, but it also mimics some short-range correlation as is revealed by the analysis of DFT exchange holes. The short-range effects result from the short-range, fine structure of the HF exchange hole (Fig. 2, close to F1) caused by the nodal surfaces and tail contributions of the orbitals (a fine structure which is not reflected by the DFT exchange hole). This leads to the somewhat surprising conclusion that approximate exchange functionals, as they are currently in use, account for both exchange, dynamic, and nondynamic correlation effects. This may explain the good performance of DFT in cases where HF and even HF-based correlation methods with some low-order correlation effects drastically fail.
2. A larger (absolute) SIE does not imply that more long-range correlation effects are covered. The magnitude of the SIE is related to the size of the regions with a positive value of the SIE-hole (Figs. 1, 2, 4), which in the case of H_2 is clearly more positive for the LDA than for the GGA (see, in particular, Fig. 1b; SIE-LDA 0.09220 hartree; SIE-GGA 0.01009 hartree); however in the case of the F_2 bonding electron pair the situation is reversed as can be anticipated from inspection of Fig. 2 (SIE-LDA 0.04464 hartree; SIE-GGA -0.09294 hartree; Table 2). The amount of the long-range correlation effect mimicked by the SIE

hole depends on the ratio between the peaks in the valence region (or at the nucleus) and the depression of the SIE hole in the bond region. This ratio is clearly larger for the GGA in the case of H_2 (see Fig. 1a and in particular Fig. 1b), while it is larger for the LDA in the case of the bonding electrons of F_2 (Fig. 2) and other molecules.

3. There are three reasons why the GGA in general covers less long-range left–right correlation. The more diffuse LDA exchange hole implies a stronger long-range left–right effect (Fig. 2). Oscillations in the GGA exchange hole reminiscent of its GEA origin partially annihilate the left–right structure of the SIE-GGA hole. The better description of the exact exchange hole close to the reference electron by GGA also reduces the strong long-range left–right structure typical of the SIE-LDA exchange hole.
4. Furthermore, it holds that the SIE of the LDA exchange generally accounts for more short-range correlation effects as can be seen from Fig. 2 (region close to F1: oscillations in the SIE-LDA hole are larger than those in the SIE-GGA hole). The improved description of the exchange hole close to the reference electron implies that fewer short-range correlation effects are mimicked by the SIE-GGA.
5. The observation that the SIE-LDA hole covers both more short-range (dynamic) and more long-range (nondynamic) correlation effects than the SIE-GGA does explains the fact that LDA functionals are more stable than GGA functionals [13, 15].

We have previously shown that a more stable DFT method, using a specific XC functional, does not necessarily lead to more accurate results (otherwise the LDA rather than the GGA approach should be the method of choice). We can extend this statement in the following way. The exchange functional leading to a larger SIE and by this to a larger amount of non-dynamic (and dynamic) electron correlation does not imply a better description of a given electron system. This becomes clear when considering that the SIE reflects features of the electronic structure as they are represented by the true intraelectronic exchange hole via the one-electron density distribution. Pair correlation effects typical of a specific electron system are missing.

On the basis of these considerations, we can draw the conclusion that it makes little sense to focus on the development of SIC exchange functionals. SIC-DFT is much too expensive and in addition suffers from the fact that interelectronic exchange is still wrongly described. On the other hand, there is hardly any systematic way to replace nonspecific by specific Coulomb correlation effects so that a more reliable description is obtained provided one wants to retain the simplicity of KS DFT. The only alternative in this situation is to develop new exchange functionals, which are optimized with regard to the electron interaction effects they cover.

Such a derivation should be based on a suitable reference set of multireference problems [dissociating molecules, biradicals, molecules with a (quasi)degenerate ground state such as Jahn–Teller systems, etc.], which

are reliably described by highly correlated wavefunction methods. The derivation could follow strategies worked out when developing hybrid orbitals, but the optimization of the exchange functional would have to be monitored by applying the analysis method described in the current work. In this way, a direct account of added/suppressed nondynamic correlation effects could be given, which in consequence would lead to a better adjustment of DFT functionals to problems with multireference character. Work is in progress to pursue and to further develop this strategy.

Acknowledgements. This work was supported financially by the Swedish Natural Science Research Council (NFR). Calculations were done on the supercomputers of Nationellt Superdatorcentrum (NSC), Linköping, Sweden. The authors thank the NSC for a generous allotment of computer time.

References

1. Hohenberg P, Kohn W (1964) *Phys Rev B* 136: 864
2. Kohn W, Sham LJ, (1965) *Phys Rev A* 140: 1133
3. (a) Parr RG, Yang W (1989) International series of monographs on chemistry 16: Density-functional theory of atoms and molecules. Oxford University Press, New York; (b) Labanowski JK, Andzelm JW (eds) Density functional methods in chemistry. (1990) Springer, Heidelberg New York Berlin; (c) Dreizler RM, Gross EKV (1990) Density functional theory. Springer Berlin Heidelberg New York; (d) Gross EKV, Dreizler RM (eds) (1995) Density functional theory. NATO ASI series B, vol 37. Plenum, New York; (e) Chong DP (ed) (1995) Recent advances in computational chemistry, vol 1. Recent advances in density functional methods, part II. World Scientific, Singapore; (f) Seminario JM, Politzer P (eds) (1996) Theoretical and computational chemistry, vol 2. Modern density functional theory – a tool for chemistry. Elsevier, Amsterdam; (g) Laird BB, Ross RB, Ziegler T (eds) (1996) Chemical applications of density functional theory. ACS symposium series 629 American Chemical Society, Washington, DC; (h) Nalewajski RF (ed) (1996) Topics in current chemistry, 180. Density functional theory I. Springer, Berlin Heidelberg New York; (i) Seminario JM (1996) Theoretical and computational chemistry, vol 4. Recent developments and applications of modern density functional theory. Elsevier, Amsterdam; (j) Joubert D (ed) (1997) Lecture notes in Physics. Density functionals: theory and applications. Springer, Berlin Heidelberg New York; (k) Springborg M (ed) (1997) Density-functional methods in chemistry and material science. Wiley, Chichester, UK; (l) Dobson JF, Vignale G, Das MP (eds) (1997) Electronic density functional theory. Recent progress and new directions. Plenum, New York; (m) Gill P (1998) In: Schleyer PvR, Allinger NL, Clark T, Gasteiger J, Kollman PA, Schaefer HF III, Schreiner PR Encyclopedia of computational chemistry, vol 1. Wiley, Chichester, UK, p 678, and references therein; (n) March NH (1992) Electron density theory of atoms and molecules. Academic New York; (p) Koch W, Holthausen MC (2000) A chemist's guide to density functional theory. Wiley, New York.
4. Slater J (1951) *Phys Rev* 81: 385
5. Becke AD (1988) *Phys Rev A* 38: 3098
6. Becke A (1995) In: Yarkony DR (ed) Advanced series in physical chemistry. Modern electronic structure theory, part II, vol 2. World Scientific, Singapore, p 1022
7. Becke A (1996) *J Chem Phys* 104: 1040
8. Gritsenko OV, Schipper PRT, Baerends EJ (1999) *J Chem Phys* 107: 5007
9. Gritsenko OV, Ensing B, Schipper PRT, Baerends EJ, (2000) *J Phys Chem A* 104: 8558
10. Handy NC, Cohen AJ (2001) *Mol Phys* 99: 403

11. He Y, Gräfenstein J, Kraka E, Cremer D (2000) *Mol Phys* 98: 1639
12. Polo V, Kraka E, Cremer D (2002) *Mol Phys* 100: 1771
13. Polo V, Kraka E, Cremer D (2002) *Theor Chem Acc* 107: 291
14. Polo V, Gräfenstein J, Kraka E, Cremer D (2002) *Chem Phys Lett* 352: 469
15. Cremer D, Filatov M, Polo V, Kraka E, Shaik S (2002) *Int J Mol Sci* 3: 604
16. Perdew JP, Zunger A, (1981) *Phys Rev B* 23: 5048
17. (a) Perdew JP In: Avery J, Dahl JP (eds) (1984) *Local density approximations in quantum chemistry and solid state physics*. Plenum, New York; (b) Perdew JP, Ernzerhof M (eds) (1998) In: Dobson JF, Vignale G, Das MP (eds) *Electronic density functional theory. Recent progress and new directions*, Plenum, New York p 31
18. (a) Pederson MR, Lin CC (1988) *J Chem Phys* 88: 1807; (b) Goedecker S, Umrigar CJ (1997) *Phys Rev A* 55: 1765; (c) Li Y, Krieger JB (1990) *Phys Rev A* 41: 1701; (d) Chen J, Krieger JB, Li Y (1996) *Phys Rev A* 54: 3939.
19. (a) Garza J, Nichols JA, Dixon DA (2000) *J Chem Phys* 112: 7880; (b) Garza J, Nichols JA, Dixon DA (2000) *J Chem Phys* 113: 6029; (c) Garza J, Vargas R, Nichols JA, Dixon DA (2001) *J Chem Phys* 114: 639
20. (a) Perdew JP, Burke K, Wang Y (1996) *Phys Rev B* 54: 16533; (b) Burke K, Perdew JP, Ernzerhof M (1998) *J Chem Phys* 109: 3760
21. (a) Schipper PRT, Gritsenko OV, Baerends EJ (1994) *Int J Quantum Chem* 52: 711; (b) Schipper PRT, Gritsenko OV, Baerends EJ (1998) *Phys Rev A* 57: 3450; (c) Schipper PRT, Gritsenko OV, Baerends EJ (1999) *J Chem Phys* 111: 4056
22. Gunnarsson O, Lundqvist BI (1976) *Phys Rev B* 31, 7588
23. Perdew JP (1985) *Phys Rev Lett* 55: 1665
24. Levy M, Perdew JP, (1985) *Phys Rev A* 32: 2010
25. Gross EKV, Dreizler RM, (1981) *Z Phys A* 302: 103
26. Perdew JP, Wang Y (1986) *Phys Rev B* 33: 8800
27. a) Perdew JP (1991) In: Ziesche P, Eschrig H (eds) *Electronic structure of solids '91*. Akademie, Berlin p 11; (b) Perdew JP, Wang Y (1992) *Phys Rev B* 45: 13244
28. Perdew JP, Burke K, Ernzerhof M (1996) *Phys Rev Lett* 77: 3865
29. Polo V, Kraka E, Cremer D *J Chem Phys* (to be published)
30. Foster JM, Boys SF (1960) *Rev Mod Phys* 32: 300
31. Vosko SH, Wilk L, Nusair M (1980) *Can J Phys* 98: 1200
32. Lee C, Yang W, Parr R (1988) *Phys Rev B* 37: 785
33. Dunning TH Jr (1989) *J Chem Phys* 99: 1007
34. (a) Huber KP, Herzberg GH (1979) *Molecular constants of diatomic molecules*. Van Nostrand-Reinhold, New York; (b) Edwards A, Goods B, Long C (1979) *J Chem Soc Faraday Trans II* 72: 984
35. Kraka E, Gräfenstein J, Gauss J, Polo V, Reichel F, Olsson L, Konkoli Z, He Z, Cremer D (2001) *Cologne 2001*. Göteborg University, Göteborg
36. March N (1987) *Phys Rev A* 36: 5077